# Neutrino physics from cosmological observations

Steen Hannestad

Department of Physics, University of Southern Denmark Campusvej 55,
DK-5230 Odense M, Denmark

**Abstract.** Cosmological observations have in the past few years become an increasingly powerful method for determining parameters within the neutrino sector, such as the presence of sterile states and the mass of neutrinos. I review the current status of the field in light of recent measurements of the cosmic microwave background by the WMAP collaboration, as well as current large scale galaxy surveys.

## 1 Introduction

Neutrinos exist in equilibrium with the electromagnetic plasma in the early universe, until a temperature of a few MeV. At this point the weak interactions freeze out and neutrinos decouple from the plasma. Shortly after this event, the temperature of the plasma falls below the electron mass, and electrons and positrons annihilate, dumping their entropy into the photon gas. This heats the photon gas while having no effect on neutrinos, and the end result is that the photon temperature is larger than the neutrino temperature by the factor $(11/4)^{1/3} \simeq 1.40$. Since the present day photon temperature has been measured with great accuracy to be 2.728 K, the neutrino temperature is known to be 1.95 K, or about $2 \times 10^{-4}$ eV. Since the heaviest neutrino has a mass of at least about 0.04 eV it must at present be extremely non-relativistic and therefore acts as dark matter. The contribution of a single neutrino species of mass $m_\nu$ to the present day matter density can be written as [1,2,3]

$$\Omega_\nu h^2 = \frac{m_\nu}{92.5\mathrm{eV}}, \tag{1}$$

so that for a neutrino mass of about 30 eV, neutrinos will make up all of the dark matter. However, this would have disastrous consequences for structure formation in the universe, because neutrinos of eV mass have very large free streaming lengths and would erase structure in the neutrino density on scales smaller than $l_{\rm fs} \simeq 1\ m_{\nu,\mathrm{eV}}^{-1}$ Gpc completely. This leads to an overall suppression of matter fluctuations at small scales, an effect which is potentially observable.

### 1.1 Absolute value of neutrino masses

The absolute value of neutrino masses are very difficult to measure experimentally. On the other hand, mass differences between neutrino mass eigenstates, $(m_1, m_2, m_3)$, can be measured in neutrino oscillation experiments. Observations

of atmospheric neutrinos suggest a squared mass difference of $\delta m^2 \simeq 3 \times 10^{-3}$ eV$^2$ [4,5,6]. While there are still several viable solutions to the solar neutrino problem from solar neutrino observations alone, the large mixing angle (LMA) solution gives by far the best fit with $\delta m^2 \simeq 5 \times 10^{-5}$ eV$^2$ [7,8]. Recently the KamLAND reactor neutrino experiment has announced a positive detection of neutrino oscillations indicating that the LMA solution is indeed correct [9].

In the simplest case where neutrino masses are hierarchical these results suggest that $m_1 \sim 0$, $m_2 \sim \delta m_{\rm solar}$, and $m_3 \sim \delta m_{\rm atmospheric}$. If the hierarchy is inverted [10,11,12,13,14,15] one instead finds $m_3 \sim 0$, $m_2 \sim \delta m_{\rm atmospheric}$, and $m_1 \sim \delta m_{\rm atmospheric}$. However, it is also possible that neutrino masses are degenerate [16,17,18,19,20,21,22,23,24,25,26], $m_1 \sim m_2 \sim m_3 \gg \delta m_{\rm atmospheric}$, in which case oscillation experiments are not useful for determining the absolute mass scale.

Experiments which rely on kinematical effects of the neutrino mass offer the strongest probe of this overall mass scale. Tritium decay measurements have been able to put an upper limit on the electron neutrino mass of 2.2 eV (95% conf.) [27]. However, cosmology at present yields an even stronger limit which is also based on the kinematics of neutrino mass. As discussed before any structure in the neutrino density below the free-streaming scale is erased and therefore the presence of a non-zero neutrino mass suppresses the matter power spectrum at small scales relative to large scale, roughly by $\Delta P/P \sim -8\Omega_\nu/\Omega_m$ [28].

This power spectrum suppression allows for a determination of the neutrino mass from measurements of the matter power spectrum on large scales, as well as the spectrum of CMB fluctuations. This matter spectrum is related to the galaxy correlation spectrum measured in large scale structure (LSS) surveys via the bias parameter, $b^2(k) \equiv P_g(k)/P_m(k)$. Such analyses have been performed several times before [29,30], most recently using data from the 2dFGRS galaxy survey [31,32,33]. These investigations found mass limits of 1.5-3 eV, depending on assumptions about the cosmological parameter space.

In a seminal paper it was calculated by Eisenstein, Hu and Tegmark that future CMB and LSS experiments could push the bound on the sum of neutrino masses down to about 0.3 eV [28]. The prospects for an absolute neutrino mass determination was discussed in further detail in Ref. [39] where it was found that in fact the upper bound could be pushed to 0.12 eV (95% conf.) using data from the Sloan Digital Sky Survey and the upcoming Planck satellite.

More recently the new WMAP data, in conjunction with large scale structure data from 2dFGRS has been used to put an upper bound on the sum of all neutrino species of $\sum m_\nu \leq 0.7$ eV (95% conf.) [34].

However, the exact value of this upper bound depends strongly on priors on other cosmological parameters, mainly $H_0$. In the present paper we calculate the upper bound on $\sum m_\nu$ from present cosmological data, with an emphasis on studying how the bound depends on the data set chosen.

In addition to their contribution to the cosmological mass density neutrinos also contribute to the cosmological energy density around the epoch of recombination. Neutrinos which have mass smaller than roughly $3T_{\rm rec}$, where $T_{\rm rec} \simeq 0.3$

eV is the temperature of recombination, will act as fully relativistic particles when it comes to CMB and large scale structure.

In the standard model there are three light neutrino species with this property. However, these particles are not necessarily in an equilibrium Fermi-Dirac distribution with zero chemical potential. It is well known that the universe contains a non-zero baryon asymmetry of the order $\eta = \frac{n_B - n_{\bar{B}}}{n_\gamma} \sim 10^{-10}$. A neutrino asymmetry of similar magnitude would have no impact on cosmology during CMB and LSS formation, but since the neutrino asymmetry is not directly observable it could in principle be much larger than the baryon asymmetry. Such a neutrino asymmetry would effectively show up as extra relativistic energy density in the CMB and LSS power spectra.

Another possibility for extra relativistic energy is that there are additional light species beyond the standard model which have decoupled early (such as the graviton or the gravitino).

From the perspective of late time evolution at $T \leq 1$ MeV it is customary to parametrize any such additional energy density in terms of $N_\nu$ [35], the equivalent number of neutrino species. In Section III we discuss bounds on $N_\nu$ from the present WMAP and 2dFGRS data, combined with additional information on other cosmological parameters from the Hubble HST key project and the Supernova Cosmology Project.

However, as will be discussed later, a non-zero neutrino chemical potential can have an effect on big bang nucleosynthesis which is profoundly different from simple relativistic energy density if it is located in the electron neutrino sector.

Another important point is that any entropy production which takes place after BBN, but prior to CMB formation will only be detectable via CMB and LSS observations. One such example is the decay of a hypothetical long-lived massive particle at temperatures below roughly 0.01 MeV.

## 2 Likelihood analysis and data sets

The extraction of cosmological parameters from cosmological data is a difficult process since for both CMB and LSS the power spectra depend on a plethora of different parameters. Furthermore, since the CMB and matter power spectra depend on many different parameters one might worry that an analysis which is too restricted in parameter space could give spuriously strong limits on a given parameter.

The most recent cosmological data is in excellent agreement with a flat $\Lambda$CDM model, the only non-standard feature being the apparently very high optical depth to reionization. Therefore the natural benchmark against which non-standard neutrino physics can be tested is a model with the following free parameters: $\Omega_m$, the matter density, the curvature parameter, $\Omega_b$, the baryon density, $H_0$, the Hubble parameter, $n_s$, the scalar spectral index of the primordial fluctuation spectrum, $\tau$, the optical depth to reionization, $Q$, the normalization of the CMB power spectrum, $b$, the bias parameter, and finally the two parameters related to neutrino physics, $\Omega_\nu h^2$ and $N_\nu$. The analysis can be restricted

to geometrically flat models, i.e. $\Omega = \Omega_m + \Omega_\Lambda = 1$. For the purpose of actual power spectrum calculations, the CMBFAST package [36] can be used.

### 2.1 LSS data

At present, by far the largest survey available is the 2dFGRS [37] of which about 147,000 galaxies have so far been analyzed. Tegmark, Hamilton and Xu [38] have calculated a power spectrum, $P(k)$, from this data, which we use in the present work. The 2dFGRS data extends to very small scales where there are large effects of non-linearity. Since we only calculate linear power spectra, we use (in accordance with standard procedure) only data on scales larger than $k = 0.2h$ Mpc$^{-1}$, where effects of non-linearity should be minimal [39]. Making this cut reduces the number of power spectrum data points to 18.

### 2.2 CMB data

The CMB temperature fluctuations are conveniently described in terms of the spherical harmonics power spectrum $C_l \equiv \langle |a_{lm}|^2 \rangle$, where $\frac{\Delta T}{T}(\theta, \phi) = \sum_{lm} a_{lm} Y_{lm}(\theta, \phi)$. Since Thomson scattering polarizes light there are additional powerspectra coming from the polarization anisotropies. The polarization can be divided into a curl-free ($E$) and a curl ($B$) component, yielding four independent power spectra: $C_{T,l}, C_{E,l}, C_{B,l}$ and the temperature $E$-polarization cross-correlation $C_{TE,l}$.

The WMAP experiment have reported data only on $C_{T,l}$ and $C_{TE,l}$, as described in Ref. [40,34,41,42,43]

We have performed the likelihood analysis using the prescription given by the WMAP collaboration which includes the correlation between different $C_l$'s [40,34,41,42,43]. Foreground contamination has already been subtracted from their published data.

In parts of the data analysis we also add other CMB data from the compilation by Wang *et al.* [44] which includes data at high $l$. Altogether this data set has 28 data points.

## 3 Numerical results

### 3.1 Neutrino masses

The analysis presented here was originally published in Ref. [45], and more details can be found there.

We have calculated $\chi^2$ as a function of neutrino mass while marginalizing over all other cosmological parameters. This has been done using the data sets described above. In the first case we have calculated the constraint using the WMAP $C_{T,l}$ combined with the 2dFGRS data, and in the second case we have added the polarization measurement from WMAP. Finally we have added the additional constraint from the HST key project and the Supernova Cosmology Project. It should also be noted that when constraining the neutrino mass it has

in all cases been assumed that $N_\nu$ is equal to the standard model value of 3.04. Later we relax this condition in order to study the LSND bound.

The result is shown in Fig. 1. As can be seen from the figure the 95% confidence upper limit on the sum of neutrino masses is $\sum m_\nu \leq 1.01$ eV (95% conf.) using the case with priors. This value is completely consistent with what is found in Ref. [46] where simple Gaussian priors from WMAP were added to the 2dFGRS data analysis. For the three cases studied we find the following limits:

| | |
|---|---|
| $\sum m_\nu < 1.01$ eV | for WMAP+Wang+2dFGRS+HST+SN-Ia |
| $\sum m_\nu < 1.20$ eV | for WMAP+Wang+2dFGRS |
| $\sum m_\nu < 2.12$ eV | for WMAP+2dFGRS |

In the middle panel of Fig. 1 we show the best fit value of $H_0$ for a given $\Omega_\nu h^2$. It is clear that an increasing value of $\sum m_\nu$ can be compensated by a decrease in $H_0$. Even though the data yields a strong constraint on $\Omega_m h^2$ there is no independent constraint on $\Omega_m$ in itself. Therefore, an decreasing $H_0$ leads to an increasing $\Omega_m$. This can be seen in the bottom panel of Fig. 1.

When the HST prior on $H_0$ is relaxed a higher value of $\sum m_\nu$ is allowed, in the case with only WMAP and 2dFGRS data the upper bound is $\Omega_\nu h^2 \leq 0.023$ (95% conf.), corresponding to a neutrino mass of 0.71 eV for each of the three neutrinos.

This effect was also found by Elgarøy and Lahav [46] in their analysis of the effects of priors on the determination of $\sum m_\nu$.

However, as can also be seen from the figure, the addition of high-$l$ CMB data from the Want *et al.* compilation also shrinks the allowed range of $\sum m_\nu$ significantly. The reason is that there is a significant overlap of the scales probed by high-$l$ CMB experiments and the 2dFGRS survey. Therefore, even though we use bias as a free fitting parameter, it is strongly constrained by the fact that the CMB and 2dFGRS data essentially cover much of the same range in $k$-space.

It should be noted that Elgarøy and Lahav [46] find that bias does not play any role in determining the bound on $\sum m_\nu$. At first this seems to contradict the discussion here, and also what was found from a Fisher matrix analysis in Ref. [32]. The reason is that in Ref. [46], redshift distortions are included in the 2dFGRS data analysis. Given a constraint on the amplitude of fluctuations from CMB data, and a constraint on $\Omega_m h^2$ , this effectively constrains the bias parameter. Therefore adding a further constraint on bias in their analysis does not change the results.

*Neutrinoless double beta decay*

Recently it was claimed that the Heidelberg-Moscow experiment yields positive evidence for neutrinoless double beta decay. Such experiments probe the 'effective electron neutrino mass $m_{ee} = |\sum_j U_{ej}^2 m_{\nu_j}|$. Given the uncertainties in the involved nuclear matrix elements the Heidelberg-Moscow result leads to a mass of $m_{ee} = 0.3 - 1.4$ eV. If this is true then the mass eigenstates are necessarily degenerate, and $\sum m_\nu \simeq 3 m_{ee}$. Taking the WMAP result of $\sum m_\nu \leq 0.70$ eV at face value seems to be inconsistent with the Heidelberg-Moscow result [47].

However, already if Ly-$\alpha$ forest data and a constraint on the bias parameter is not used in the analysis the upper bound of $\sum m_\nu \leq 1.01$ eV is still consistent. For this reason it is probably premature to rule out the claimed evidence for neutrinoless double beta decay.

### 3.2 Neutrino relativistic energy density

For the case of the effective number of neutrino species we have in all cases calculated constraints in the $(\Omega_b h^2, N_\nu)$ plane, while marginalizing over all other parameters. The reason for this is that for Big Bang Nucleosynthesis purposes these are exactly the important parameters. Therefore, to combine CMB, LSS, and BBN constraints the marginalization over $\Omega_b h^2$ should not be performed. Furthermore, when constraining $N_\nu$ we have always assumed that $\sum m_\nu \simeq 0$ so that the neutrino mass has no influence on cosmology.

We start out by investigating constraints on $N_\nu$ from CMB and LSS data alone. In Fig. 2 we show $\Delta\chi^2$ for a global fit to $N_\nu$ which marginalizes over all other cosmological parameters. The overall best fit for the WMAP $T$ and $TE$ data, combined with the Wang *et al.* compilation, the 2dFGRS data, the HST key project data on $H_0$, as well as the SNI-a data on $\Omega_m$, has $\chi^2 = 1467.6$ for a total of 1395 degrees of freedom. This gives $\chi^2/\text{d.o.f.} = 1.05$ which is entirely compatible with the best fit WMAP value for the standard $\Lambda$CDM model of $\chi^2/\text{d.o.f.} = 1.066$. We also show constraints for two other analyses. The first is for WMAP and 2dFGRS data alone and the second for WMAP data alone. The bounds for the three cases are

$N_\nu = 4.0^{+3.0}_{-2.1}$ for WMAP+Wang+2dFGRS+HST+SN-Ia
$N_\nu = 3.1^{+3.9}_{-2.8}$ for WMAP+2dFGRS
$N_\nu = 2.1^{+6.7}_{-2.2}$ for WMAP only

These bound are entirely compatible with those found by Crotty, Lesgourgues and Pastor [50], and much tighter than the pre-WMAP constraints.

The constraints derived here are also compatible with what is found by Pierpaoli [49], where are assumption of spatial flatness was relaxed.

In the lower panels of Fig. 2 we show the best fit values of $H_0$ and $\Omega_m$ for a given value of $N_\nu$. The main point to note is that the constraint on $N_\nu$ is strongly dependent on $H_0$. This was also found in Ref. [51]. With only CMB data and the weak top-hat prior on $H_0$ the bound on $N_\nu$ is very weak. Adding the HST Key Project prior on $H_0$ cut away a significant amount of parameter space both at low and high $N_\nu$. Adding the 2dFGRS and Wang *et al.* data mainly has the effect of shifting the best fit value to higher $N_\nu$, but also cuts away the low $N_\nu$ values, an effect also seen in Ref. [50].

In Fig. 3 we show constraints on $(\Omega_b h^2, N_\nu)$ for the full data set described above. The best fit value for $\Omega_b h^2$ is 0.0233, which is equivalent to the value found in the WMAP data analysis. In the 2-dimensional plots the 68% and 95% regions are formally defined by $\Delta\chi^2 = 2.30$ and 6.17 respectively. Note that this means that the 68% and 95% contours are not necessarily equivalent to the same confidence level for single parameter estimates.

It should be noted here that in addition to an upper bound on $N_\nu$ there is also a $3.0\sigma$ confidence detection of $N_\nu > 0$. This is in concordance with the pre-WMAP data from which a non-trivial lower bound on $N_\nu$ could also be derived.

*Adding BBN information* – In the case where all the relativistic energy density contained in $N_\nu$ is produced prior to BBN, a BBN constraint can be added to the CMB and LSS constraint without any problems. In practice we have used abundances of He-4 and D to make constraints in the $(\Omega_b h^2, N_\nu)$ plane. We use the following values for the primordial abundances [53,54] $\mathrm{D/H} = 2.78^{+0.44}_{-0.38} \times 10^{-5}$ and $\mathrm{Y}_P = 0.238 \pm 0.005$

This calculation is shown in Fig. 4. In terms of a single parameter constraint on $N_\nu$ it is $N_\nu = 2.6^{+0.4}_{-0.3}$ (95 % conf.). Compared to the recent calculation by Abazajian [52] of a BBN-only constraint of $1.7 \leq N_\nu \leq 3.5$ (95 % conf.) this is a significant improvement. Very interestingly the new limit suggests the possibility that $N_\nu$ is actually less than 3. This is for instance possible in scenarios with extremely low reheating temperature [55,56]. Note that this result is also consistent with the calculation by Barger et al. [57], although t heir preferred region is slightly different because they do not include large scale structure data in their analysis.

Of course this conclusion is mainly based on the fact that CMB and LSS data prefers a slightly higher value of $\Omega_b h^2$ than BBN. It should also be stressed that the estimates of the primordial abundances could be biased by systematic effects so that the quoted statistical error bar is not really meaningful. Therefore it is probably premature to talk of any inconsistency between the $N_\nu = 3$ prediction of the standard model and observations.

In fact the argument can also be reversed. If $N_\nu$ is fixed to the standard model value of 3 then then CMB and LSS constraint on $\Omega_b h^2$ provides an accurate measurement of primordial He-4. Using the derived constraint on $\Omega_b h^2$ the 95% confidence range for $Y_P$ is $0.2458 \leq Y_P \leq 0.2471$. This could point to a serious underlying systematic effect in observational determinations of $Y_P$, as discussed in Ref. [58].

### 3.3 Combining $\sum m_\nu$ with $N_\nu$ - constraining LSND

From the analyses in the above two sections it was found that: *(a)* An increasing $\sum m_\nu$ can be compensated by a decreasing $H_0$ and *(b)* An increasing $N_\nu$ can be compensated by an increasing $H_0$. One might therefore wonder whether a model with non-zero $\sum m_\nu$, combined with $N_\nu > 3$ can provide a good fit to the data.

In order to test this we have performed a likelihood analysis for $\sum m_\nu$ for different values of $N_\nu$. We show this in Fig. 5. This analysis was performed with all available data and priors.

As can be seen from the figure, the best fit actually is actually shifted to higher $\sum m_\nu$ when $N_\nu$ increases, and the conclusion is that a model with high neutrino mass and additional relativistic energy density can provide acceptable fits to the data. As a function of $N_\nu$ the upper bound on $\sum m_\nu$ is (at 95% confidence)

$\sum m_\nu \leq 1.01$ eV for $N_\nu = 3$
$\sum m_\nu \leq 1.38$ eV for $N_\nu = 4$
$\sum m_\nu \leq 2.12$ eV for $N_\nu = 5$

This has significant implications for attempts to constrain the LSND experiment using the present cosmological data. Pierce and Murayama conclude from the present MAP limit that the LSND result is excluded [47] (see also Ref. [48]).

However, for several reasons this conclusion does not follow trivially from the present data. In general the three mass differences implied by Solar, atmospheric and the LSND neutrino measurements can be arranged into either 2+2 or 3+1 schemes. Recent analyses [59] of experimental data have shown that the 2+2 models are ruled out. The 3+1 scheme with a single massive state, $m_4$, which makes up the LSND mass gap, is still marginally allowed in a few small windows in the $(\Delta m^2, \sin^2 2\theta)$ plane. These gaps are at $(\Delta m^2, \sin^2 2\theta) \simeq (0.8\,\mathrm{eV}^2, 2\times10^{-3}), (1.8\,\mathrm{eV}^2, 8\times10^{-4}), (6\,\mathrm{eV}^2, 1.5\times10^{-3})$ and $(10\,\mathrm{eV}^2, 1.5\times10^{-3})$. These four windows corresponds to masses of $0.9, 1.4, 2.5$ and $3.2$ eV respectively. From the Solar and atmospheric neutrino results the three light mass eigenstates contribute only about 0.1 eV of mass if they are hierarchical. This means that the sum of all mass eigenstate is close to $m_4$.

The limit for $N_\nu = 4$ which corresponds roughly to the LSND scenario is $\sum m_\nu \leq 1.4$ eV, which still leaves the lowest of the remaining windows. The second window at $m \sim 1.8$ eV is disfavoured by the data, but not at very high significance.

## 4 Discussion

We have calculated improved constraints on neutrino masses and the cosmological relativistic energy density, using the new WMAP data together with data from the 2dFGRS galaxy survey.

Using CMB and LSS data together with a prior from the HST key project on $H_0$ yielded an upper bound of $\sum m_\nu \leq 1.01$ eV (95% conf.). While this excludes most of the parameter range suggested by the claimed evidence for neutrinoless double beta decay in the Heidelberg-Moscow experiment, it seems premature to rule out this claim based on cosmological observations.

Another issue where the cosmological upper bound on neutrino masses is very important is for the prospects of directly measuring neutrino masses in tritium endpoint measurements. The successor to the Mainz experiment, KATRIN, is designed to measure an electron neutrino mass of roughly 0.2 eV, or in terms of the sum of neutrino mass eigenstates, $\sum m_\nu \leq 0.75$ eV. The WMAP result of $\sum m_\nu \leq 0.7$ eV (95% conf.) already seems to exclude a positive measurement of mass in KATRIN. However, this very tight limit depends on priors, as well as Ly-$\alpha$ forest data, and the more conservative present limit of $\sum m_\nu \leq 1.01$ eV (95% conf.) does not exclude that KATRIN will detect a neutrino mass.

From the data we also inferred a limit on $N_\nu$ of $N_\nu = 4.0^{+3.0}_{-2.1}$ (95% conf.) on the equivalent number of neutrino species. This is a marked improvement over the previous best limit of roughly $N_\nu \leq 13$ [51,60].

When light element measurements of He-4 and D are included the bound is strengthened considerably to $N_\nu = 2.6^{+0.4}_{-0.3}$ (95 % conf.). Interestingly this suggests a possible value of $N_\nu$ which is *less* than 3. This could be the case for instance in scenarios with very low reheating temperature where neutrinos were never fully equilibrated [55,56]. However, it should be stressed that primordial abundances could be dominated by systematics. Therefore it is probably premature to talk of a new BBN "crisis".

Finally, we also found that the neutrino mass bound depends on the total number of light neutrino species. In scenarios with sterile neutrinos this is an important factor. For instance in 3+1 models the mass bound increases from 1.0 eV to 1.4 eV, meaning that the LSND result is not ruled out by cosmological observations yet.

## References


1. S. Hannestad and J. Madsen, Phys. Rev. D **52**, 1764 (1995) [arXiv:astro-ph/9506015].
2. A. D. Dolgov, S. H. Hansen and D. V. Semikoz, Nucl. Phys. B **503**, 426 (1997) [arXiv:hep-ph/9703315].
3. G. Mangano, G. Miele, S. Pastor and M. Peloso, arXiv:astro-ph/0111408.
4. S. Fukuda *et al.* [Super-Kamiokande Collaboration], Phys. Rev. Lett. **85**, 3999 (2000) [arXiv:hep-ex/0009001].
5. N. Fornengo, M. C. Gonzalez-Garcia and J. W. Valle, Nucl. Phys. B **580** (2000) 58 [arXiv:hep-ph/0002147].
6. M. Maltoni, T. Schwetz, M. A. Tortola and J. W. Valle, arXiv:hep-ph/0207227.
7. See the SNO homepage http://sno.phy.queensu.ca
8. J. N. Bahcall, M. C. Gonzalez-Garcia and C. Pena-Garay, arXiv:hep-ph/0204314.
9. K. Eguchi *et al.* [KamLAND Collaboration], Phys. Rev. Lett. **90**, 021802 (2003) [arXiv:hep-ex/0212021].
10. V. A. Kostelecky and S. Samuel, Phys. Lett. B **318**, 127 (1993).
11. G. M. Fuller, J. R. Primack and Y. Z. Qian, Phys. Rev. D **52**, 1288 (1995) [arXiv:astro-ph/9502081].
12. D. O. Caldwell and R. N. Mohapatra, Phys. Lett. B **354**, 371 (1995) [arXiv:hep-ph/9503316].
13. S. M. Bilenky, C. Giunti, C. W. Kim and S. T. Petcov, Phys. Rev. D **54**, 4432 (1996) [arXiv:hep-ph/9604364].
14. S. F. King and N. N. Singh, Nucl. Phys. B **596**, 81 (2001) [arXiv:hep-ph/0007243].
15. H. J. He, D. A. Dicus and J. N. Ng, arXiv:hep-ph/0203237.
16. A. Ioannisian and J. W. Valle, Phys. Lett. B **332**, 93 (1994) [arXiv:hep-ph/9402333].
17. P. Bamert and C. P. Burgess, Phys. Lett. B **329**, 289 (1994) [arXiv:hep-ph/9402229].
18. R. N. Mohapatra and S. Nussinov, Phys. Lett. B **346**, 75 (1995) [arXiv:hep-ph/9411274].
19. H. Minakata and O. Yasuda, Phys. Rev. D **56**, 1692 (1997) [arXiv:hep-ph/9609276].
20. F. Vissani, arXiv:hep-ph/9708483.
21. H. Minakata and O. Yasuda, Nucl. Phys. B **523**, 597 (1998) [arXiv:hep-ph/9712291].

22. J. R. Ellis and S. Lola, Phys. Lett. B **458**, 310 (1999) [arXiv:hep-ph/9904279].
23. J. A. Casas, J. R. Espinosa, A. Ibarra and I. Navarro, Nucl. Phys. B **556**, 3 (1999) [arXiv:hep-ph/9904395].
24. J. A. Casas, J. R. Espinosa, A. Ibarra and I. Navarro, Nucl. Phys. B **569**, 82 (2000) [arXiv:hep-ph/9905381].
25. E. Ma, J. Phys. G **25**, L97 (1999) [arXiv:hep-ph/9907400].
26. R. Adhikari, E. Ma and G. Rajasekaran, Phys. Lett. B **486**, 134 (2000) [arXiv:hep-ph/0004197].
27. J. Bonn *et al.*, Nucl. Phys. Proc. Suppl. **91**, 273 (2001).
28. W. Hu, D. J. Eisenstein and M. Tegmark, Phys. Rev. Lett. **80**, 5255 (1998) [arXiv:astro-ph/9712057].
29. R. A. Croft, W. Hu and R. Dave, Phys. Rev. Lett. **83**, 1092 (1999) [arXiv:astro-ph/9903335].
30. M. Fukugita, G. C. Liu and N. Sugiyama, Phys. Rev. Lett. **84**, 1082 (2000) [arXiv:hep-ph/9908450].
31. Ø. Elgarøy *et al.*, arXiv:astro-ph/0204152.
32. S. Hannestad, arXiv:astro-ph/0205223.
33. A. Lewis and S. Bridle, arXiv:astro-ph/0205436.
34. D. N. Spergel *et al.*, astro-ph/0302209
35. G. Steigman, D. N. Schramm and J. E. Gunn, Phys. Lett. B **66**, 202 (1977).
36. U. Seljak and M. Zaldarriaga, Astrophys. J. **469**, 437 (1996).
37. J. Peacock *et al.*, Nature **410**, 169 (2001).
38. M. Tegmark, A. J. S. Hamilton and Y. Xu, arXiv:astro-ph/0111575
39. S. Hannestad, arXiv:astro-ph/0211106.
40. C. L. Bennett *et al.*, astro-ph/0302207
41. A. Kogut *et al.*, astro-ph/0302213
42. G. Hinshaw *et al.*, astro-ph/0302217
43. L. Verde, *et al.*, astro-ph/0302218
44. X. Wang, M. Tegmark, B. Jain and M. Zaldarriaga, arXiv:astro-ph/0212417.
45. S. Hannestad, JCAP **0305**, 004 (2003) [arXiv:astro-ph/0303076].
46. Ø. Elgarøy and O. Lahav, astro-ph/0303089.
47. A. Pierce and H. Murayama, arXiv:hep-ph/0302131.
48. C. Giunti, arXiv:hep-ph/0302173.
49. E. Pierpaoli, arXiv:astro-ph/0302465.
50. P. Crotty, J. Lesgourgues and S. Pastor, arXiv:astro-ph/0302337.
51. S. Hannestad, Phys. Rev. D **64**, 083002 (2001) [arXiv:astro-ph/0105220].
52. K. N. Abazajian, arXiv:astro-ph/0205238.
53. D. Kirkman *et al.*, astro-ph/0302006
54. K. A. Olive, G. Steigman and T. P. Walker, Phys. Rept. **333**, 389 (2000) [arXiv:astro-ph/9905320].
55. G. F. Giudice, E. W. Kolb and A. Riotto, Phys. Rev. D **64**, 023508 (2001) [arXiv:hep-ph/0005123].
56. M. Kawasaki, K. Kohri and N. Sugiyama, Phys. Rev. D **62**, 023506 (2000) [arXiv:astro-ph/0002127].
57. V. Barger, J. P. Kneller, H. S. Lee, D. Marfatia and G. Steigman, Phys. Lett. B **566**, 8 (2003) [arXiv:hep-ph/0305075].
58. R. H. Cyburt, B. D. Fields and K. A. Olive, arXiv:astro-ph/0302431.
59. M. Maltoni, T. Schwetz, M. A. Tortola and J. W. Valle, Nucl. Phys. B **643**, 321 (2002) [arXiv:hep-ph/0207157].
60. S. Hannestad, Phys. Rev. Lett. **85**, 4203 (2000) [arXiv:astro-ph/0005018].

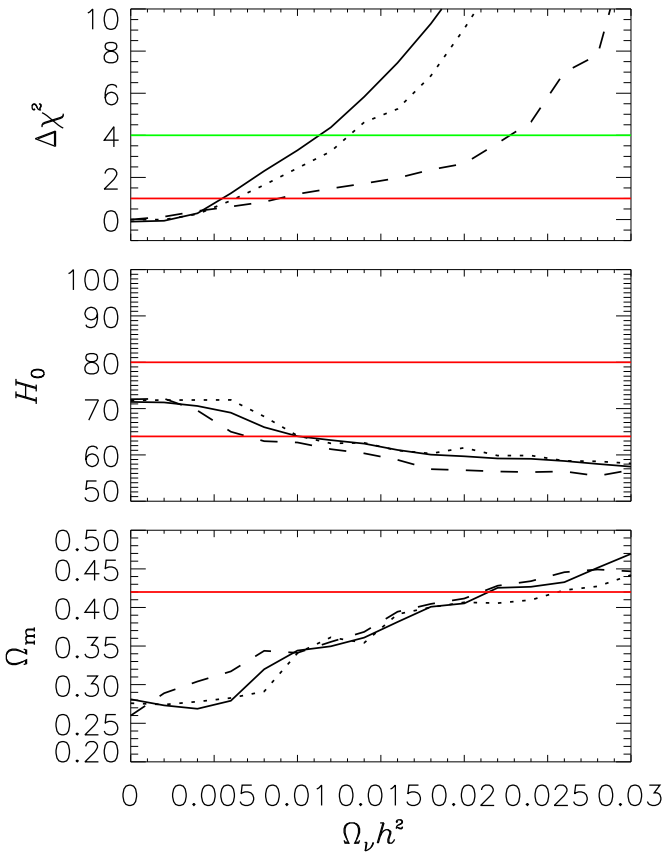


**Fig. 1.** The top panel shows $\chi^2$ as a function of $\sum m_\nu$ for different choices of priors. The dotted line is for WMAP + 2dFGRS data alone, the dashed line is with the additional Wang *et al.* data. The full line is for additional HST and SNI-a priors as discussed in the text. The horizontal lines show $\Delta\chi^2 = 1$ and 4 respectively. The middle panel shows the best fit values of $H_0$ for a given $\sum m_\nu$. The horizontal lines show the HST key project $1\sigma$ limit of $H_0 = 72 \pm 8$ km s Mpc$^{-1}$. Finally, the lower panel shows best fit values of $\Omega_m$. In this case the horizontal line corresponds to the SNI-a $1\sigma$ upper limit of $\Omega_m < 0.42$.

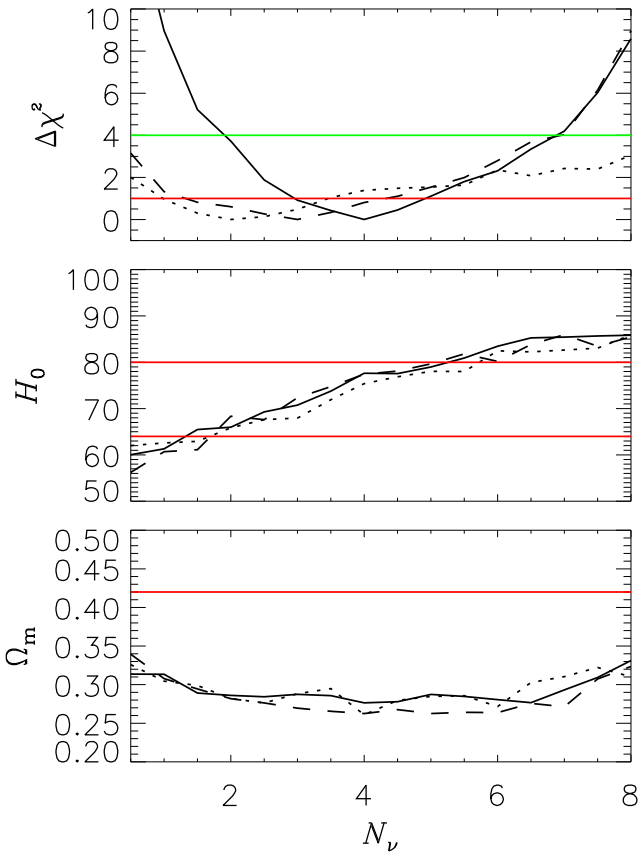


**Fig. 2.** $\chi^2$ as a function of $\sum N_\nu$ for different choices of priors. The dotted line is for WMAP data alone, the dashed line is with the additional Wang *et al.* and 2dFGRS data. The full line is for additional HST and SNI-a priors as discussed in the text.The horizontal lines show $\Delta\chi^2 = 1$ and 4 respectively. The middle panel shows the best fit values of $H_0$ for a given $N_\nu$. The horizontal lines show the HST key project $1\sigma$ limit of $H_0 = 72 \pm 8$ km s Mpc$^{-1}$. Finally, the lower panel shows best fit values of $\Omega_m$. In this case the horizontal line corresponds to the SNI-a $1\sigma$ upper limit of $\Omega_m < 0.42$.

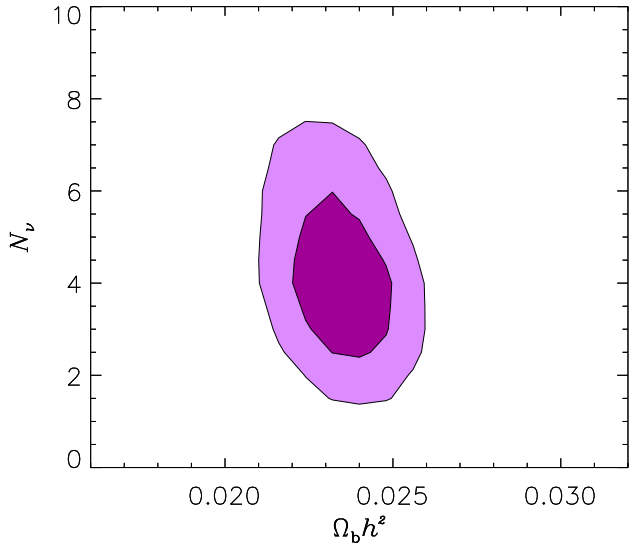


**Fig. 3.** 68% and 95% confidence contours in the $(\Omega_b h^2, N_\nu)$ plane for the WMAP TT and TE data, combined with the 2dFGRS data, the HST data on $H_0$ and the SNI-a data on $\Omega_m$.

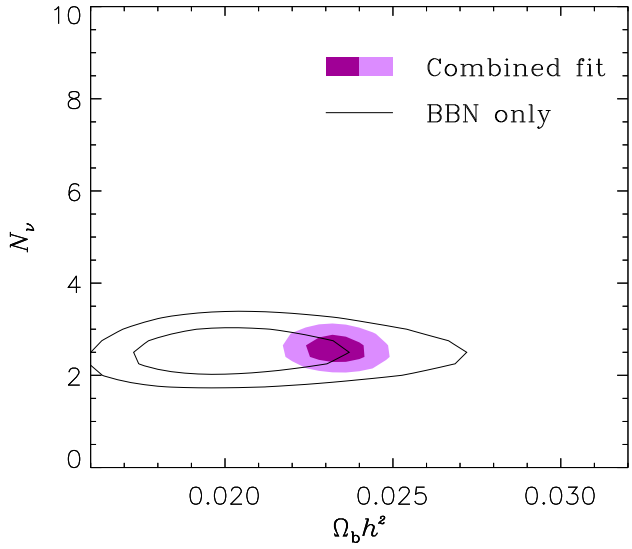


**Fig. 4.** 68% and 95% confidence contours in the $(\Omega_b h^2, N_\nu)$ plane for the same data sets as in fig. 3, but with the addition of BBN data. The lined contours are the 68% and 95% regions for BBN data alone.

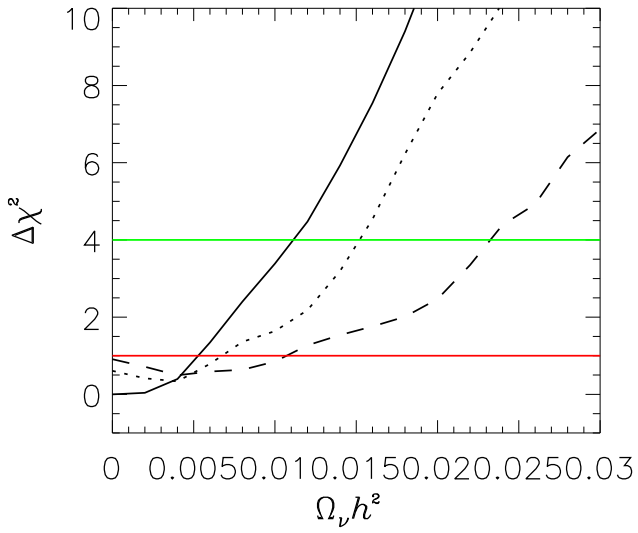


**Fig. 5.** $\Delta\chi^2$ as a function of $\sum m_\nu$ for various different values of $N_\nu$. The full line is for $N_\nu = 3$, the dotted for $N_\nu = 4$, and the dashed for $N_\nu = 5$. $\Delta\chi^2$ is calculated relative to the best fit $N_\nu = 3$ model.